Engineering Solid Mechanics 11 (2023) 103-118

Contents lists available at GrowingScience

Engineering Solid Mechanics

homepage: www.GrowingScience.com/esm

Kenaf-Coir based hybrid nano-composite: an analytical and representative volume element analysis

Shikha Parashar[a]* and V. K. Chawla[a]

[a]*Department of Mechanical and Automation Engineering, IGDTUW, Delhi, 110006, India*

A R T I C L E I N F O

Article history:
Received 18 January 2022
Accepted 26 June 2022
Available online
14 August 2022

Keywords:
Coir
Elastic Properties
Green-Composite
Kenaf
Representative Volume Element

A B S T R A C T

The increasing demand for good and improved polymeric composites has led to a surge in the number of researches on hybrid composites, strengthened and enforced with the natural fibres. This paper mainly analyses and presents the attributes of hybrid composites made from natural fibres and carbon nano-tube (CNT) nanoparticles. A novel hybrid composite considered in this research includes kenaf and coir fibres with CNT nanoparticles embedded in an epoxy matrix. The proposed hybrid nanocomposite's elastic features are calculated by using different analytical models like Chamis, Mori-Tanaka, Nielson elastic models etc and also with the help of Representative Volume Element Analysis (RVE). The content of fibre volume is varied in four different samples and it is found that upon varying the content of fibre volume, the mechanical properties like longitudinal modulus and transverse modulus got affected. The results evaluated from different analytical models are observed to be in good agreement with each other and also with the results of RVE analysis.

1. Introduction

Fibre-reinforced composite (FRC) is a growing area of research in different areas of engineering because of its high strength, good resistance to wear, high modulus, and less weight (Ayatollahi & Aliha, 2008; Aliha et al., 2018; Rout & Satapathy, 2012). A natural fibre reinforced composite mainly inculcates within it a matrix of polymer implanted along with natural filaments of high strength, for example, rice husk, sisal, wood dust, kenaf, cellulose, starch, coconut, areca, banana, and coir (Ku et al., 2011; Kumar et al., 2014). These attributes of natural fibres are encouraging the researchers to traverse the field of fibre composites, green production and sustainability (Aliha et al., 2018; Gupta et al., 2022; Geethammaa et al., 2005; Parashar & Chawla, 2021, 2022; Saxena & Chawla, 2021, 2022; Sadik et al., 2020, Kumar et al., 2020). Additionally, the FRC material can be used in the form of fillers for the creation of polymeric composites because of their easy availability around the year (Zhao et al., 2008; Adeniyi et al., 2019, 2021).

In the previous few years, there has been a tremendous increase in the study of nano polymer reinforced natural fibre composites. Various nanoparticles have been utilized by different researchers during their studies on nano-composites. Mainly the nano-fillers like nano-silica, nano-clay, nano-titanium particles, and carbon nanotubes, are mixed with the matrix to improve their mechanical properties such as toughness, strength, stiffness, thermal properties etc. But these properties of nano-composites also rely upon many other factors like the size of the nanoparticle, volume content of the nanoparticle added, dispersion of nano-fillers, as well as their compatibility with matrices and the fibres, and the interface fastening in between them. In case the bonding between nanoparticle and polymer matrix is weak, it may lead to a decrease in the stress transfer and lower the performance of the nano-composites.

* Corresponding author.
E-mail addresses: shikha001phd18@igdtuw.ac.in (S. Parashar)

ISSN 2291-8752 (Online) - ISSN 2291-8744 (Print)

doi: 10.5267/j.esm.2022.8.001

The fibre reinforced polymer composites (FRPC) are extensively modelled by finite element modelling (FEA), to find the various properties of materials owing to their easy and efficient application in the designing sector. Seidel & Lagoudas (2006) applied the Mori–Tanaka technique, and self-consistent method to find the properties of carbon nanotubes reinforced material. The authors examined the impact of a layer of interphase in the middle of the polymer matrix and nanotubes and saw that at a lesser volume fraction, it extraordinarily affected the transverse characteristics of the proposed composite. A 2D image analysis is proposed by Sadik et al. (2020) for the measurement of the orientation of short fibres in the polymer composites. A thermo-graphic technique is proposed by Amali & McLaughlin (2013) for the identification and analysis of failures in composite materials. A numerical homogenisation technique is introduced by Theocaris et al. (1997) to report the modulus of elasticity in the transverse direction of composite material. The authors reported that the state of the fibre cross-sectional area affects the general flexibility moduli.

The forecasts of the thermostatic characteristics of a composite material reinforced with small un-aligned fibre-glass are analysed and reported by Lusti et al. (2002). The authors applied a finite element analysis along with exploratory estimations in their study. The transverse, longitudinal thermal coefficients and elastic modulus in the longitudinal direction are found to be in good agreement with the numerical results. To examine the effect of varying aspect ratio, volume fraction, and distribution of fibres according to fibre length on the thermo-elastic characteristics of FRC, a mathematical strategy is proposed by Hine et al. (2002). The authors used boundary conditions and the Monte-Carlo method for the development of spherical cylinders to deliver an arbitrary morphology. The authors reported the outcome of applied analytical models in synergy with the numerical results. Anumandla & Gibson (2006) analysed composites reinforced with CNTs by using a micromechanics model and reported the elastic modulus of the proposed composite material in their work. The proposed model represented the one-dimensional, three-dimensional arbitrary organization of the nanotubes and nanotube's bend, along with the length of the nanotubes. The effect of montmorillonite (MMT) nanoparticle addition to hybrid composites reinforced with kenaf/coir fibres is studied by Islam et al. (2015). Prabhudass & Palanikumar (2021) worked on finding the consequences of fibre treatment on thermal and mechanical features of kenaf-coir based epoxy composites. Kari et al. (2007) used a homogenization analytical model to evaluate the composite material developed with randomly dispersed short fibres in the transverse direction. The research carried out by various authors on kenaf fibre hybrid composites and nano-composites is summarised in Table 1.

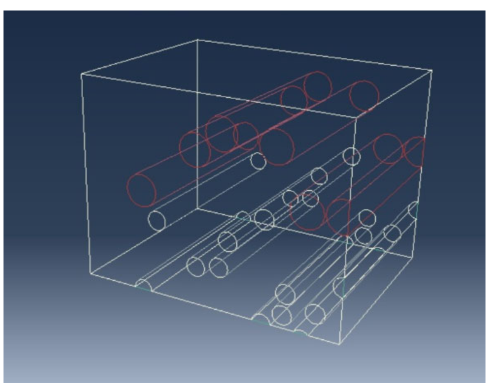

Fig. 1. Representative Volume Element with circular fibres

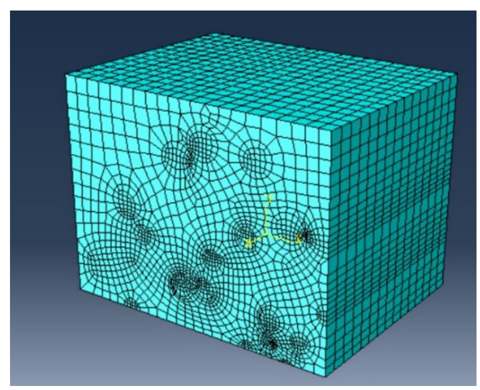

Fig. 2. RVE meshing

Table 1. Literature stated on kenaf fibre reinforced hybrid composites as well as nanocomposites

Composite	***Filler Reinforcements***	***References***
Kenaf and phenolic resin	Leaf fibre of Pineapple treated by silane	Asim et al. (2018)
Kenaf/ Aloe vera fibre/ PLA	Montmorillonite (MMT) clay	Ramesh et al. (2020)
Kenaf / epoxy	Nanoparticles of Silica	Bajuri et al. (2016)
	Nanofiller of Oil Palm	Saba et al. (2016)
	Kevlar fibres	Yahaya et al. (2014)
	Carbon nanotubes (CNTs)	Sapiai et al. (2015)
Kenaf / polylactic acid	Corn Flour	Kwon et al. (2014)
	Coir and Bamboo fibres	Yusoff et al. (2016)
Kenaf / polyester resin	Banana fiber	Alavudeen et al. (2015)
	Glass fibres	Hashemi et al. (2018)
	Glass fibres	Ghani et al. (2012)
Kenaf / polypropylene grafted by maleic anhydride	Graphene Nanoplatelets	Idumah et al. (2017)
Kenaf/polypropylene	Wool fibres/ Ammonium Polyphosphate	Subasinghe et al. (2018)
	Graphene Nanoplatelets	Idumah and Hassan (2016)

The impact of hybrid loading of fillers on polyester composite reinforced with glass-jute fibres is analysed by Kumar et al. (2021). The properties and characteristics of an asphalt mix by mixing kenaf and coir fibres are reported by Sani et al. (2011). The authors mentioned that the features and behaviour of hot mixed asphalt became better with the addition of kenaf and coir fibres. Similar studies are performed by Aziz & Hamid (2018) and they found that the impact resistance and mechanical properties of concrete are improved after mixing it with a combination of kenaf and coir fibres. The properties of kenaf and coir are observed to be opposite to each other, the kenaf fibre was found to have high water absorption capacity and high tensile strength whereas, coir fibre is observed to be better in ductility and exhibits low tensile strength.

In the literature, several nano-fillers and their effect on various properties of fibre composites are also reported. Accordingly, the properties of the carbon nanotubes (CNT) are reported by Iijima (1991). The author observed that the inclusion of CNTs improves the electrical, mechanical and thermal properties of the composites.

In the hybrid composites, mainly two techniques are applied to utilize CNTs in the hybrid composites namely (1) Engrossing the CNT developed filaments, and (2) Engrossing of CNTs into the element matrix. In the former criteria, it is observed that the carbon nanotubes improve the interface transfer of load among the matrices and fibres of the composite, whereas in the latter criteria they are found to improve the properties of the matrix (Rana et al., 2013, El-Moumen et al., 2017). CNTs are aligned inside the framework of the polymer composite material and the effective damping behaviour of the proposed composite material is reported by Jangam et al., (2016). The composite with varying volume fractions of CNTs is investigated by Tarfaoui et al., (2016). They evaluated the volume fraction content of CNTs and mentioned the development in the characteristics of composite having more than one fibre. The shear strength of the glass-CNT-epoxy nano-composite is reported by Godara et al. (2010).

From the literature, it is seen that several authors have worked on coir based composite material and evaluated its properties, but no work is observed on hybrid composite material having coir fibre, kenaf fibre and carbon nanotubes in combination. And, accordingly, a potential research gap is evident to evaluate the mechanical properties of the aforementioned hybrid composite material. Given the aforesaid research gap, in the present research, an attempt is carried out to develop and model a novel hybrid composite material by using kenaf and coir fibres with CNT nanoparticles, embedded in an epoxy matrix. The proposed hybrid nanocomposite's elastic features are then calculated by using different analytical models like Chamis, Mori-Tanaka, Nielson elastic models etc. The pre-eminent motive of this research is to observe the development in the mechanical properties of the proposed hybrid composite material by changing the volume content of the fibres. Additionally, a 3D micromechanical representative volume component (RVE) with round cross segments of fibres, used in the hybrid composite is modelled by using ABAQUS CAE and analysis is carried out for the same. A basic structure of the representative volume element showing fibres with a circular cross-section is shown in figure 1. The meshing of the proposed RVE model is shown in Fig. 2.

2. Methodology

2.1 Material composition

The matrix in the proposed hybrid composite material is composed of epoxy, coir fibre, and kenaf fibre, and carbon nanotubes are considered nano-filler. The reinforced fibres are considered to be homogenous and isotropic. The properties of different constituents of the proposed hybrid composite material are mentioned in Table 2.

Table 2. Properties of different constituents of proposed hybrid composite material

Material	*Young's Modulus (GPa)*	*Tensile Strength (MPa)*	*Diameter (μm)*	*Poisson's Ratio (μ)*
Coir fibre	5	175	15	0.3
Kenaf fibre	53	930	25	0.342
Epoxy	3.81	65	-	0.41
CNTs	1200	40000	D = 10 - 20 nm, L = 0.5 - 2 μm	0.28

Table 3. Various compositions of the hybrid composite

Code	*Sample*	*Epoxy, wt.%*	*Kenaf, wt.%*	*Coir, wt.%*	*CNT, wt.%*
S1	E/KF/CF	70	15	15	0
S2	E/KF/CF/CNF0.75	69.25	15	15	0.75
S3	E/KF/CF/CNT1	69	15	15	1
S4	E/KF/CF/CNT3	67	15	15	3

Four samples of proposed hybrid composite materials are considered for modelling and analysis. In Table 3 details of the composition of samples for the proposed hybrid composite material are mentioned. Samples are developed with varying volume content of carbon nanotubes (CNT) percentage inside the kenaf, coir and epoxy-based hybrid composite.

3. Analytical model

Analytical modelling applies numerical expressions and equations to anticipate the properties of the composite. Therefore, analytical models namely Mori Tanaka, Halpin-Tsai, Nielson Elastic, and Chamis are applied in this study to anticipate the effective elastic properties of the proposed hybrid composite material.

3.1 Halpin Tsai model

A mathematical model to derive and anticipate the mechanical properties of a composite material was proposed by Halpin and Tsai, (1967). Their model has been described below:

Longitudinal Properties:

$$E_1 = E_f S_f + E_m S_m \quad (1)$$

Transverse properties:

$$\frac{E_C}{E_m} = \frac{1+\eta\xi S_f}{1-\eta S_f} \quad (2)$$

$$\eta = \frac{\frac{E_f}{E_m} - 1}{\frac{E_f}{E_m} + \xi} \quad (3)$$

$$\xi = 2X\frac{l}{d} \quad (4)$$

In which,

$E_1, E_C, and\ E_m$ represents the longitudinal modulus, composite modulus and matrix modulus respectively.

S_f represents volume fraction of fibres

E_f, d, l represents the Modulus of fibre, diameter, and length of the fibres subsequently.

From the literature, it is observed that the Halpin-Tsai application has some limitations to the composite material built up with two sizes and classes of reinforcements. Hence, in this paper, a modified and altered Halpin-Tsai (H-T) model is established considering that the reinforcement in the proposed hybrid composite material is evenly scattered.

$$\frac{E_{m'}}{E_m} = \frac{3}{8}\left\{\frac{1+(\xi_{KF}\,\eta_{KF\_L}S_{KF})}{1-\eta_{KF\_L}\,S_{KF}}\right\} + \frac{5}{8}\left\{\frac{1+(2\eta_{KF\_T}S_{KF})}{1-\eta_{KF\_T}S_{KF}}\right\} \quad (5)$$

$$\eta_{KF\_L} = \left\{\frac{(E_{KF}\,/\,E_m) - 1}{(E_{KF}\,/\,E_m) + \xi_{KF}}\right\} \quad (6)$$

$$\eta_{KF\_T} = \left\{\frac{(E_{KF}\,/\,E_m) - 1}{(E_{KF}\,/\,E_m) + 2}\right\} \quad (7)$$

$$\xi_{KF} = 2\left\{\frac{l_{KF}}{d_{KF}}\right\} \quad (8)$$

where,

$E_{m'}$, E_m represents the modulus of kenaf fibre and matrix respectively.
ξ_{KF} represents the curve fitting parameter that depends on fibre packing geometry.
η_{KF} represents the stress partitioning factor
S_{KF} represents the volume fraction of the kenaf fibres.
"L" and "T" represent the longitudinal and transverse sides.
l_{KF}, d_{KF} represents the length and diameter of the kenaf fibres

The micro-geometry of multiscale reinforcements is different, the Halpin-Tsai model is modified according to the fibres and carbon nanotubes. The 3/8 and 5/8 are the corresponding coefficients for weightage. The symbol m' is the KFs/EP composite, and maybe referred to afresh matrix. So, the modulus of elasticity in the case of CNTs/afresh matrix as:

$$\frac{E_{m''}}{E_{m'}} = \frac{3}{8}\left\{\frac{1+(\xi_{CF}\,\eta_{CF\_L}S_{CF})}{1-\eta_{CF\_L}\,S_{CF}}\right\} + \frac{5}{8}\left\{\frac{1+(2\eta_{CF\_T}S_{CF})}{1-\eta_{CF\_T}S_{CF}}\right\} \quad (9)$$

$$\eta_{CF\_L} = \left\{\frac{(E_{CF}\,/\,E_{m'}) - 1}{(E_{CF}\,/\,E_{m'}) + \xi_{CF}}\right\} \quad (10)$$

$$\eta_{CF\_T} = \left\{\frac{(E_{CF} / E_{m'}) - 1}{(E_{CF} / E_{m'}) + 2}\right\} \quad (11)$$

$$\xi_{CF} = 2\left\{\frac{l_{CF}}{d_{CF}}\right\} \quad (12)$$

where,

$E_{m''}$ relates to the composite's young's modulus — new matrix KFs/CFs/EP, E_{CF} represents the modulus of elasticity of coir fibres, S_{CF} represents the coir fibres volumetric fraction, l_{CF} represents the coir fibres length of the, d_{CF} represents coir fibres diameter. Post this step, m'' is the CFs/KFs/EP hybrid composite, taken as an additional new matrix. Therefore, the modulus of elasticity of CNTs/additional afresh matrix is now seen as

$$\frac{E_{m'''}}{E_{m''}} = \frac{3}{8}\left\{\frac{1 + (\xi_{CNT}\,\eta_{CNT\_L} S_{CNT})}{1 - \eta_{CNT\_L}\,S_{CNT}}\right\} + \frac{5}{8}\left\{\frac{1 + (2\eta_{CNT\_T} S_{CNT})}{1 - \eta_{CNT\_T} S_{CNT}}\right\} \quad (13)$$

$$\eta_{CNT\_L} = \left\{\frac{(E_{CNT} / E_{m''}) - 1}{(E_{CNT} / E_{m''}) + \xi_{CNT}}\right\} \quad (14)$$

$$\eta_{CNT\_T} = \left\{\frac{(E_{CNT} / E_{m''}) - 1}{(E_{CNT} / E_{m''}) + 2}\right\} \quad (15)$$

$$\xi_{CNT} = 2\left\{\frac{l_{CNT}}{d_{CNT}}\right\} \quad (16)$$

where $E_{m'''}$ is the modulus of elasticity of overall composite afresh matrix CNTs/CFs/KFs/EP. E_{CNT} represents the CNTs modulus of elasticity, S_{CNT} represents the volumetric fraction of carbon nanotubes, d_{CNT} symbolises the average diameter of carbon nanotubes, and l_{CNT} represents the average length of the carbon nanotubes. The new Halpin-Tsai model in the case of multiscale composites is represented as:

$$E_C = E_m\left[\frac{3}{8}\left\{\frac{1 + (\xi_{KF}\,\eta_{KF\_L} S_{KF})}{1 - \eta_{KF\_L}\,S_{KF}}\right\} + \frac{5}{8}\left\{\frac{1 + (2\eta_{KF\_T} S_{KF})}{1 - \eta_{KF\_T} S_{KF}}\right\}\right] \times \left[\frac{3}{8}\left\{\frac{1 + (\xi_{CF}\,\eta_{CF\_L} S_{CF})}{1 - \eta_{CF\_L}\,S_{CF}}\right\} + \frac{5}{8}\left\{\frac{1 + (2\eta_{CF\_T} S_{CF})}{1 - \eta_{CF\_T} S_{CF}}\right\}\right] \times \left[\frac{3}{8}\left\{\frac{1 + (\xi_{CNT}\,\eta_{CNT\_L} S_{CNT})}{1 - \eta_{CNT\_L}\,S_{CNT}}\right\} + \frac{5}{8}\left\{\frac{1 + (2\eta_{CNT\_T} S_{CNT})}{1 - \eta_{CNT\_T} S_{CNT}}\right\}\right] \quad (17)$$

3.2 Nielson elastic model

The Nielson elastic model is developed with the addition ϕ_{max}, (maximum packing fraction) i.e. a function of the model's geometry. The value of the packing fraction is considered 0.785, with the placement of circular fibres within the square array (Sudheer et al., 2015).

Longitudinal Properties:

$$E_1 = E_{f1}S_{f1} + E_{f2}S_{f2} + E_m S_m \quad (18)$$

where,

E_1, E_2 = Longitudinal modulus of the composite, Transverse modulus of the composite respectively.
E_{f1}, E_{f2}, E_m = Elastic modulus of both the fibres and matrix respectively
S_{f1}, S_{f2}, S_m = The volume fraction of both the fibres and matrix respectively.
ϕ_{max} = Maximum packing fraction.

Transverse properties:

$$E_2 = E_m\left(\frac{1 + \eta\zeta S_f}{1 + \eta\psi S_f}\right) \quad (19)$$

where,

$$\eta = \frac{\frac{E_f}{E_m} - 1}{\frac{E_f}{E_m} + \zeta} \quad (20)$$

$$\zeta = 2$$

$$\psi = 1 + \left(\frac{1 - \phi_{max}}{\phi_{max}^2}\right) S_f \quad (21)$$

ζ represents the shape factor i.e., the aspect ratio and the filler orientation
ψ is related to the volume fraction of the fibres
ϕ is associated with the packing density of the fillers.

In the case of coir and kenaf fibres with the incorporation of carbon nano-tube particles, this equation is modified, in which the subscript K_f represents kenaf fibre and C_f represents the coir fibre and *m* represents the matrix:

Longitudinal property:

$$E_1 = E_{Kf}S_{Kf} + E_{Cf}S_{Cf} + E_mS_m \quad (22)$$

Transverse property:

$$E_2 = E_m\left(\frac{1 + \eta_{Kf}\zeta S_{Kf} + \eta_{Cf}\zeta S_{Cf}}{1 + \eta_{Kf}\psi_{Kf}S_{Kf} + \eta_{Cf}\psi_{Cf}S_{Cf}}\right) \quad (23)$$

where,

$$\eta_{Kf} = \frac{\frac{E_{Kf}}{E_m} - 1}{\frac{E_{Kf}}{E_m} + \zeta} \quad (24)$$

$$\eta_{Cf} = \frac{\frac{E_{Cf}}{E_m} - 1}{\frac{E_{Cf}}{E_m} + \zeta} \quad (25)$$

$$\zeta = 2$$

$$\psi_{Kf} = 1 + \left(\frac{1 - \phi_{max}}{\phi_{max}^2}\right) S_{Kf} \quad (26)$$

$$\psi_{Cf} = 1 + \left(\frac{1 - \phi_{max}}{\phi_{max}^2}\right) S_{Cf} \quad (27)$$

3.3 Mori-Tanaka model

The Mori-Tanaka model was proposed by Mori and Tanaka, (1973). The model exhibits a rational approach and an effective field theory for inhomogeneity in an infinite medium, to relate the average fibre stress and fibre strain, with the matrix medium (Mishra & Das, 2020). The Mori-Tanaka approach is modelled as follows:

$$E_1 = S_f E_1^f + (1 - S_f)E_m + 2S_f(1 - S_f)Z_1(\nu_{12}^f - \nu^m)^2 \quad (28)$$

$$E_2 = \frac{E_1}{[1 - (\nu^m)^2]\,(y_1 + y_2)} \quad (29)$$

$$\nu_{12} = \nu^m + 2S_f\frac{Z_1}{E^m}(\nu_{12}^f - \nu_m)\,[1 - (\nu^m)^2] \quad (30)$$

where,

$$y_1 = S_f Z_1(\frac{E_1^f}{E^m})\left[\frac{1 + \nu^m}{E_m} - \frac{2}{E_1^f} + \frac{1 + \nu_{23}^f}{E_2^f}\right] \quad (31)$$

$$y_2 = \frac{1}{1-(\nu^m)^2} + 2S_f\left(\frac{E_1}{Z_2}\right)\left[1+\nu_{23}^f - \frac{E_2^f}{E^m}(1-\nu^m)\right] \quad (32)$$

$$Z_1 = \left\{-2\,(1-S_f)\frac{(\nu_{23}^f)^2}{E_1^f} + (1-S_f)\frac{1-\nu_{23}^f}{E_2^f} + (1+\nu^m)\frac{[1+S_f(1-2\nu^m)]}{E_m^m}\right\}^{-1} \quad (33)$$

E_1, E_2, E_m = Longitudinal modulus of the composite, Transverse modulus of the composite, Matrix modulus respectively.
S_f, S_m = The volume fraction of the fibres and matrix respectively.
ν^f, ν^m= Poisson's ratio of fibres, matrix respectively.

3.4 Chamis model

The Chamis model (Chamis & Sendeckyj, 1968) is a semi-empirical model for evaluating the self-reliant elastic properties of composite material. In this paper, the Chamis model is transformed by using the rule of mixtures and substituting the fibre volume fraction with its square root (Sudheer et al., 2015).

Longitudinal properties:

$$E_1 = E_f S_f + E_m S_m \quad (34)$$

$$\nu_C = \nu_f S_f + \nu_m S_m \quad (35)$$

Transverse properties:

$$E_2 = \frac{E_m}{1-\left\{\sqrt{S_f}\left[1-\left(\frac{E_m}{E_f}\right)\right]\right\}} \quad (36)$$

where,

E_1, E_2, E_m = Longitudinal modulus of the composite, Transverse modulus of the composite, Matrix modulus respectively.
S_f, S_m = The volume fraction of the fibres and matrix respectively.
ν_C, ν_f, ν_m= Poisson's ratio of composite, fibres, and matrix respectively.

For the composite embodied in this research, the Chamis model is modified as:

$$E_1 = E_{Kf} S_{Kf} + E_{Cf} S_{Cf} + E_m S_m \quad (37)$$

$$E_2 = \frac{E_m}{1-\left\{\sqrt{S_{Kf}}\left[1-\left(\frac{E_m}{E_{Kf}}\right)\right]\right\}} + \frac{E_m}{1-\left\{\sqrt{S_{Cf}}\left[1-\left(\frac{E_m}{E_{Cf}}\right)\right]\right\}} \quad (38)$$

3.5 The prospective multivariate modelling approach

The approach applied here for modelling consists of homogenization with two steps. The first step focuses on analysing the potential characteristics of the nanoparticle composite. This paved the way to compute the functional properties of nanoparticles. The effective nano-particles matrix was then treated to be included in the second step, consisting of different analytical and numerical techniques for homogenization and for gaining the complete elastic features of the proposed hybrid composite material. As the first step, the nanoparticle taken here is carbon nanotubes (CNTs). The modulus of elasticity is computed according to the modified rule of mixtures given by Tsai and Hahn (2018) as:

$$E_{p,11} = \phi E_{np} + (1-\phi)E_m = E_{p,33} \quad (39)$$

$$E_{p,22} = \frac{E_{np}E_m}{\phi E_m + (1-\phi)E_{np} + \phi(1-\phi)\beta E_{np}E_m} \quad (40)$$

where,

$$\beta = \frac{\nu_{np}^2 E_m/E_{np} + \nu_m^2 E_{np}/E_m - 2\nu_{np}\nu_m}{\phi E_m + (1-\phi)E_{np} + \phi(1-\phi)\beta E_{np} E_m} \quad (41)$$

where,

ϕ is the effective volume fraction of the nanoparticle

E_p, E_{np}, E_m represents the elastic modulus of the particulate composite, nanoparticle, and matrix respectively.

ν_{np}, ν_m= Poisson's ratio of nanoparticle, matrix respectively

The different analytical models presented above have been thoroughly analysed for the proposed kenaf-coir based hybrid composite material. The values are calculated by varying the content of nanoparticles in the proposed hybrid composite. The volume of nanoparticle content is varied from 0%, 0.75%, 1% and 3% (Sapiai et al., 2015, Ramesh et al., 2020). The effective elastic properties (transverse modulus, longitudinal modulus, Poisson's ratio) for the proposed hybrid composite material calculated for different volume fractions from the application of different analytical models are mentioned below in Tables 4, 5, 6 and 7 respectively and, are shown in form of bar graphs in Fig. 13, Fig. 14 and Fig. 15.

4. Representative volume element analysis

The representative volume element (RVE) analysis for composites is referred to as the minimal volume on which any measurement is made to be done, that produces a result depictive of the complete model. The RVE analysis is performed using ABAQUS software version 6.14, to determine the elastic features of the kenaf coir hybrid composite (Barbero, 2013). The following assumptions are made for the composite model:

i. The composite material is taken to be free from voids and any other holes or irregularities.

ii. Fibres are assumed to be randomly distributed inside the matrix.

iii. A perfect bonding exists between the fibres and the matrix.

iv. The RVE is meshed using the hexahedra method with a mesh size of 0.00005.

4.1 Virtual Domain

The virtual domain for our RVE is as follows:

- 3 Dimensional System.
- Unidirectional Composite
- Cubic RVE of size:
  - Length = 160 µm,
  - Width = 160 µm

4.2 Number of fibres within the RVE window

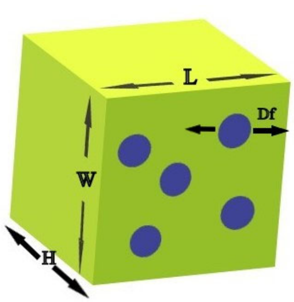

$$V_f = \frac{N\pi {D_f}^2 H}{4LWH}$$

$$N = \frac{4LWV_f}{\pi {D_f}^2}$$

Table 5. EasyPBC Parameters for RVE

Parameters	Kenaf fibres	Coir fibres
Volume fraction of fibres (V_f)	0.20	0.20
Diameter (D_f)	25 µm	15 µm
Length (L)	160 µm	160 µm
Width (W)	80 µm	80 µm

For the number of kenaf fibres in the RVE Window,

$$N_{kf} = \frac{4 \times 160 \times 80 \times 0.20}{\pi \times (25)^2} = 5.21$$

For the number of coir fibres in the RVE Window,

$$N_{kf} = \frac{4 \times 160 \times 80 \times 0.20}{\pi \times (15)^2} = 14.5$$

This hybridization is based on microscale modelling of hybrid Natural fibre composites called Kenaf Coir fibre hybrid composite.

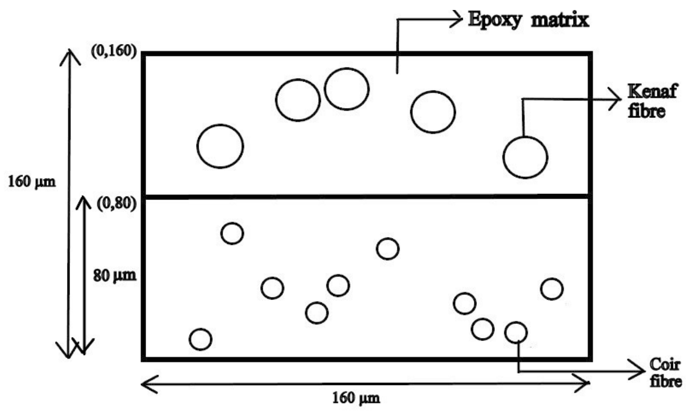

Fig. 3. RVE showing hybridization of fibres

Fig. 1 depicts the RVE model of the hybrid composite proposed in this research. Fig. 3 shows the hybridization of fibres, along with the number of fibres to be inculcated in the RVE window. Based on this hybridization, the RVE model has been developed in ABAQUS.

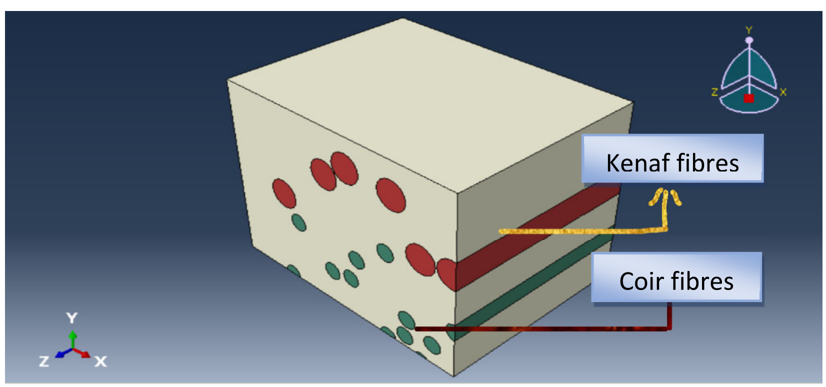

Fig. 4. Fibres dispersed in the matrix

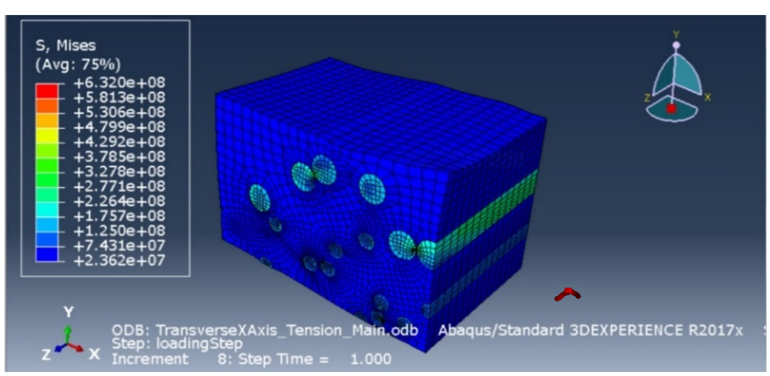

Fig. 5. Transverse modulus after processing, according to Von Mises Criteria

Fig. 4 portrays the RVE element with different fibres dispersed in the matrix content. Fig. 5 and Fig. 6 represent the deformation of RVE on the application of transverse loading. It has been observed that the fibres remain intact, whereas the matrix gets deformed. Fig. 7 depicts the in-plane shear modulus after processing, according to Von-Mises criteria. Fig. 8 and Fig. 9 represent the Principal Stresses S11 and S22 respectively, on the application of in-plane shear stresses. Fig. 10 depicts the resultant displacement U, after the application of inplane shear stresses. Fig. 11 and Fig. 12 depict the longitudinal loading after processing according to von-mises and max principal stress criteria respectively.

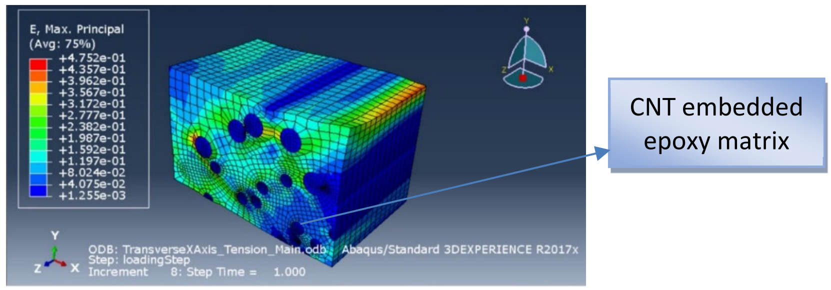

Fig. 6. Transverse modulus after processing, according to maximum principal stress criteria

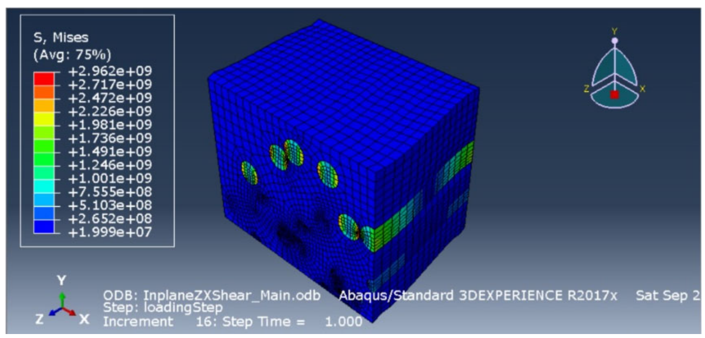

Fig. 7. In-plane shear modulus after processing, according to Von-Mises criteria

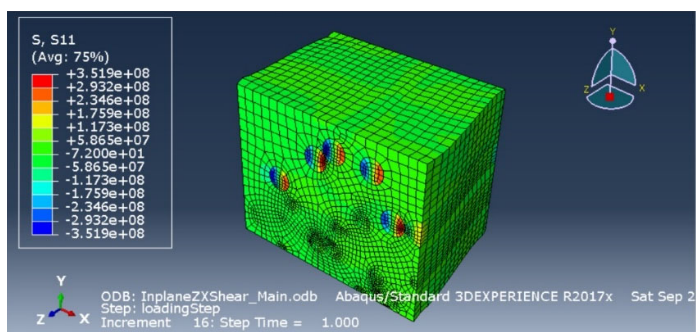

Fig. 8. Principal Stress S11, after application of in-plane shear stress

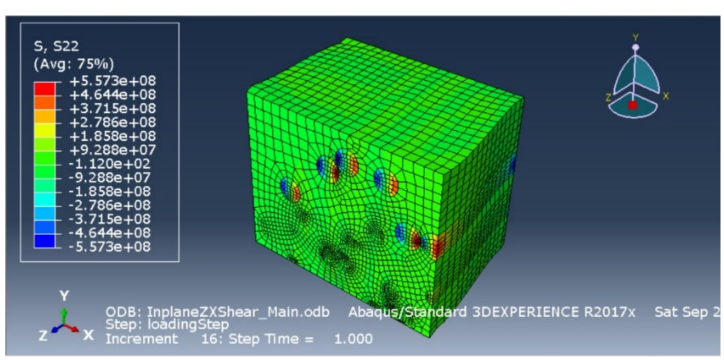

Fig. 9. Principal Stress S22, after application of in-plane shear stress

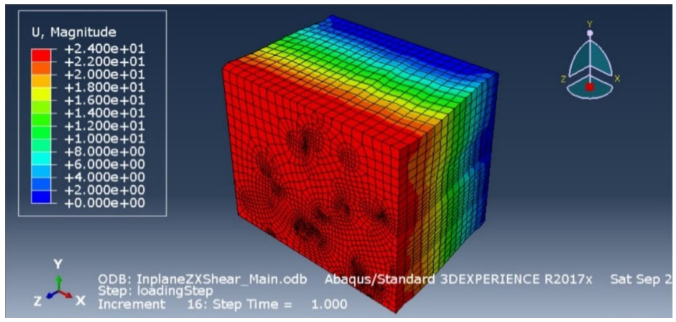

Fig. 10. Resultant Displacement U, after application of in-plane shear stress

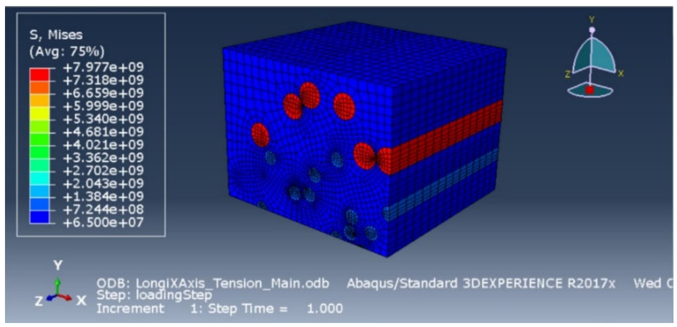

Fig. 11. Longitudinal modulus after processing, according to Von-Mises Criteria

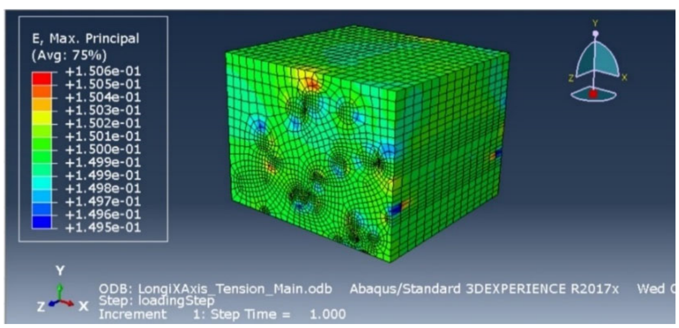

Fig. 12. Longitudinal modulus after processing, according to Maximum principal stress theory

5. Results and Discussions

5.1 Modulus at differing fibre volume content

The modulus in the longitudinal direction, at a differing volume content, for different analytical models is shown in Tables 3, 4, 5 and 6. Also, it can be seen from the graph (Fig. 4) that as the percentage of nanoparticles in the hybrid composite is increased from 0% to 0.75%, 0.75-1%, and 1-3%, the longitudinal modulus is also observed to increase. Also, results are observed for an increase in the Transverse Modulus on increasing the fibre volume fraction from 0 to 3%. In the case of Poisson's ratio, it is observed that as the content of fibre is increased, the Poisson's ratio is seen to decrease.

5.2 Effect of varying volume content on elastic properties

The effect of varying the volume fraction of fibres is observed, on the elastic properties of the composite like Longitudinal modulus, Transverse Modulus and Poisson's ratio. In Fig. 4, the varying fibre fraction effect on longitudinal modulus has been observed for the composites as shown. The results obtained from various analytical models like Halpin–Tsai, Chamis Model, Nielsen Elastic and Mori Tanaka have been correlated and are seen to be in good compliance with each other. Figure 4 depicts that a directly proportional relation exists between the fibre volume fraction and longitudinal modulus. Thus, as the content of nanofiber is decreased, the longitudinal modulus also decreases. This may be ascribed to the fact that as the CNTs increase the rigidity of the composite also increases.

The effect of varying the volume content of fibres is also seen in the Transverse modulus. Transverse modulus is referred to as the scale of stress in the transverse direction to the strain in that direction. Fig. 3 depicts the fibre fraction effect on the transverse modulus of hybrid nanocomposites. In the figure, the transverse modulus is evaluated according to the fibre fraction content of the composite and it has been observed that the Transverse modulus is directly proportional to the varying fraction of fibres in the composite.

The effect of varying the volume content of fibres is also seen in Poisson's Ratio. It is the measure of lateral strain to the longitudinal strain, measured in the direction of the applied force. It has been observed according to figure 5 that the Poisson's ratio is inversely proportional to the fibre volume content, and decreases as the content of CNTs decrease in the composite.

5.3 RVE at varying volume content

RVE analysis has been done on the kenaf coir hybrid composite and results have been analysed for varying volume content of carbon nanotube particles in the composite using ABAQUS module. It has been observed that on increasing the content of nanoparticles in the hybrid composite, the Transverse modulus and Longitudinal modulus have been found to increase, whereas the Poisson's ratio has been found to decrease, in comparison to the existing literature (Ramesh et al., 2020).

Table 4. at 0 % CNT content (S1)

Models/Properties	Halpin Tsai Model	Nielson Elastic Model	Chamis Model	Mori-Tanaka Model	RVE	Deviation (%)
Transverse Modulus (GPa)	10.1198	10.0635	10.1090	10.0754	10.4136	0.420
Longitudinal Modulus (GPa)	11.3670	11.3670	11.3670	11.390	11.5269	0.066
Poisson Ratio (μ)	0.3935	0.3935	0.3935	0.3942	0.3964	0.056

Table 5. at 0.75% CNT content (S2)

Models/Properties	Halpin Tsai Model	Nielson Elastic Model	Chamis Model	Mori-Tanaka Model	RVE	Deviation (%)
Transverse Modulus (GPa)	11.1880	11.0820	11.1530	11.1290	11.4110	0.590
Longitudinal Modulus (GPa)	17.4669	17.4669	17.4669	17.4849	18.1184	0.033
Poisson Ratio (μ)	0.3832	0.3832	0.3832	0.3817	0.3932	0.126

Table 6. at 1% CNT content (S3)

Models/Properties	Halpin Tsai Model	Nielson Elastic Model	Chamis Model	Mori-Tanaka Model	RVE	Deviation (%)
Transverse Modulus (GPa)	11.5910	11.4830	11.4980	11.5540	11.8319	0.680
Longitudinal Modulus (GPa)	19.7400	19.7400	19.7400	19.6920	19.5263	0.080
Poisson Ratio (μ)	0.3823	0.3823	0.3823	0.3799	0.4039	0.206

Table 7. at 3% CNT content (S4)

Models/Properties	Halpin Tsai Model	Nielson Elastic Model	Chamis Model	Mori-Tanaka Model	RVE	Deviation (%)
Transverse Modulus (GPa)	11.8380	11.7810	11.8390	11.8150	11.9915	0.476
Longitudinal Modulus (GPa)	36.4869	36.4869	36.4869	36.3741	37.8632	0.170
Poisson Ratio (μ)	0.3805	0.3805	0.3805	0.3801	0.3915	0.080

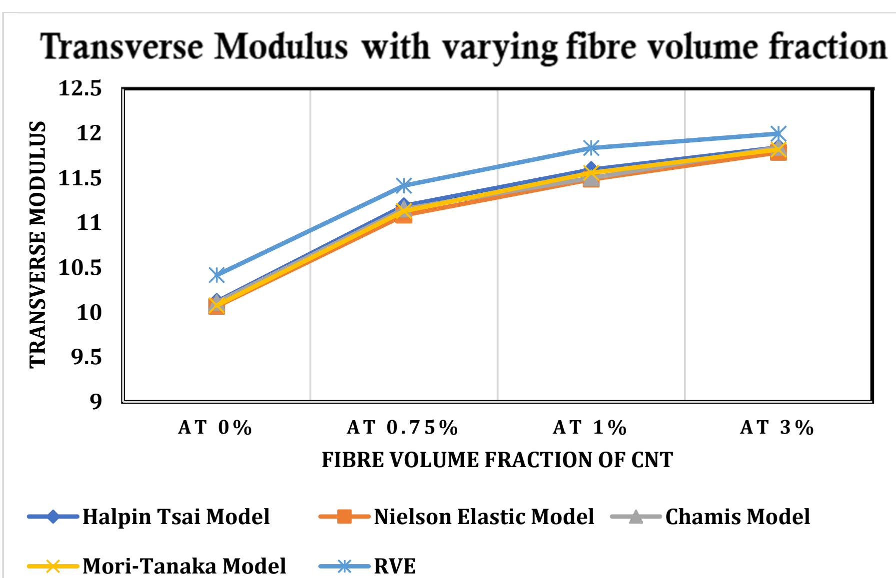

Fig. 13. Transverse modulus variation

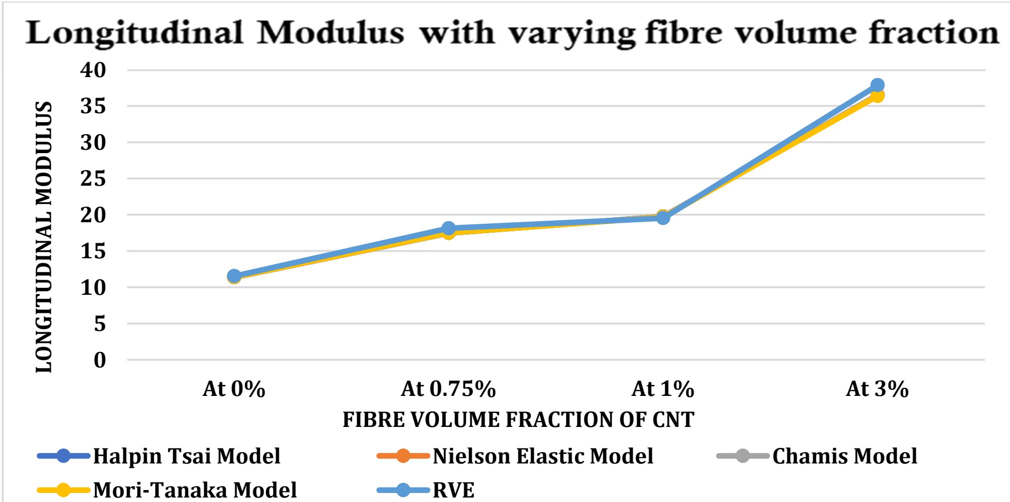

Fig. 14. Longitudinal modulus variation

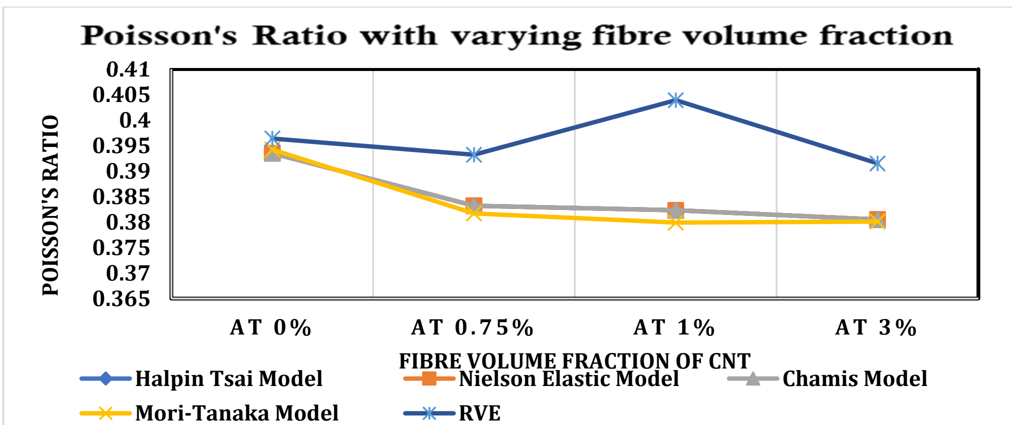

Fig. 15. Poisson's ratio variation

The Modulus is seen to have increased from 4.5 GPa to 10.1198 GPa at 0% CNT content, 3.3 GPa to 11.59 GPa at 1% CNT and from 3.4 GPa to 11.838 GPa at 3% CNT Content, in comparison to the previously available literature, as shown in Fig.16. Therefore, it can be seen that on increasing the content of CNT, the modulus is also found to increase. The results have also been compared with the existing literature and found that the present composite has a better modulus and strength in comparison to the other composites as shown in Fig.16.

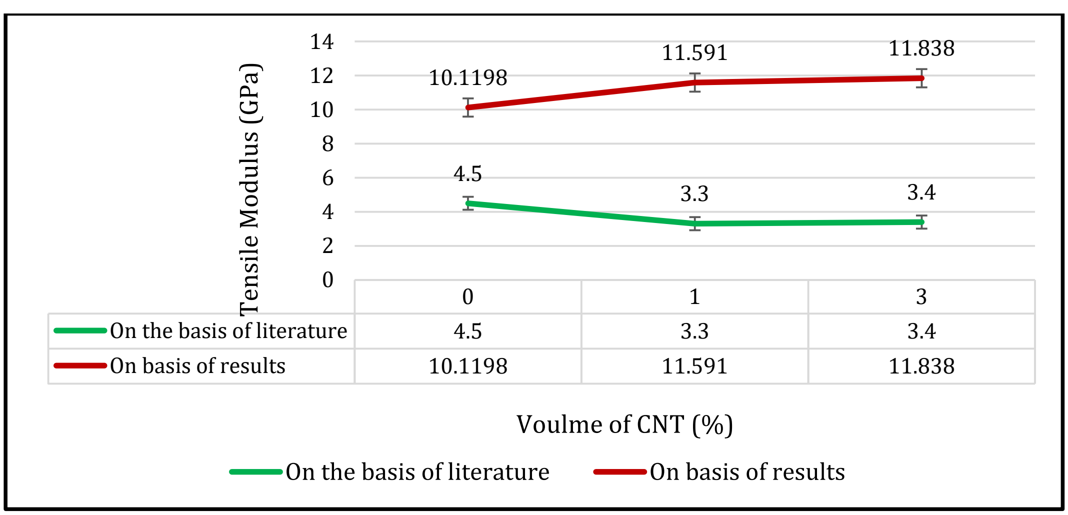

Fig. 16. Comparison with previous literature (Ramesh et al., 2020)

6. Conclusion

This paper presents four analytical mechanical models for calculating and predicting the elastic characteristics of nanoparticle kenaf coir hybrid composites. The models incurred here in the paper are namely, the Mori-Tanaka, Halpin Tsai, Nielson Elastic and Chamis Model. The outcomes of all the above models are found to be in good agreement with each other. Representative Volume Element analysis has also been carried out for kenaf coir composite. The effective properties of kenaf coir-based hybrid CNT nanocomposite have been analysed based on the varying volume fraction of the Carbon nanotube particles between 0 to 3%. The following conclusions drawn from it have been illustrated below:

- The effect of varying volume fractions of fibre particles has been observed on mechanical properties like transverse modulus, longitudinal modulus, and Poisson's ratio. These properties have been calculated from various analytical and mathematical models used for analysing hybrid nano-composites and using the RVE analysis.
- Out of all the four analytical models implied, Halpin Tsai Model is observed to provide the best results for the above-considered hybrid composite.
- The three-dimensional representative volume element has been developed, with a random distribution of the fibres in the matrix using ABAQUS CAE, and the mechanical properties like transverse modulus, longitudinal modulus, and Poisson's ratio have been analysed.
- The results of the four analytical models, Halpin Tsai model, Chamis model, Mori-tanaka model, Nielson elastic model for finding the mechanical properties of the fibre composite, are found to be in good agreement with the results of RVE analysis.

References

Adeniyi, A. G., Adeoye, S. A., Onifade, D. V., & Ighalo, J. O. (2021). Multi-scale finite element analysis of effective elastic property of sisal fiber-reinforced polystyrene composites. *Mechanics of Advanced Materials and Structures*, *28*(12), 1245-1253.

Adeniyi, A. G., Ighalo, J. O., & Onifade, D. V. (2019). Banana and plantain fibre-reinforced polymer composites. *Journal of Polymer Engineering*, *39*(7), 597-611.

Alavudeen, A., Rajini, N., Karthikeyan, S., Thiruchitrambalam, M., & Venkateshwaren, N. (2015). Mechanical properties of banana/kenaf fibre-reinforced hybrid polyester composites: Effect of woven fabric and random orientation. *Materials & Design (1980-2015), 66,* 246-257.

Aliha, M. R. M., Razmi, A., & Mousavi, A. (2018). Fracture study of concrete composites with synthetic fibres additive under modes I and III using ENDB specimen. *Construction and Building Materials*, *190*, 612-622.

Amali, R., & McLaughlin, D. (2013). Failure identification in composite materials using Thermographic method. *Engineering Solid Mechanics*, *1*(2), 37-42.

Anumandla, V., & Gibson, R. F. (2006). A comprehensive closed-form micromechanics model for estimating the elastic modulus of nanotube-reinforced composites. *Composites Part A: Applied Science and Manufacturing*, *37*(12), 2178-2185.

Asim, M., Paridah, M. T., Saba, N., Jawaid, M., Alothman, O. Y., Nasir, M., & Almutairi, Z. (2018). Thermal, physical properties and flammability of silane treated kenaf/pineapple leaf fibres phenolic hybrid composites. *Composite Structures, 202,* 1330-1338.

Ayatollahi, M. R., & Aliha, M. R. M. (2008). Mixed-mode fracture analysis of polycrystalline graphite–a modified MTS criterion. *Carbon*, *46*(10), 1302-1308.

Aziz, A. N. A., & Hamid, R. (2018). Mechanical properties and impact resistance of hybrid kenaf and coir fibre reinforced concrete. *Journal of Advanced Research in Applied Mechanics*, *47*(1), 1-10.

Bajuri, F., Mazlan, N., Ishak, M. R., & Imatomi, J. (2016). Flexural and compressive properties of hybrid kenaf/silica nanoparticles in the epoxy composite. *Procedia Chemistry, 19,* 955-960.

Barbero, E. J. (2013). *Finite element analysis of composite materials using AbaqusTM* (Vol. 2103). Boca Raton: CRC press.

Chamis, C. C., & Sendeckyj, G. P. (1968). Critique on theories predicting thermoelastic properties of fibrous composites. *Journal of Composite Materials*, *2*(3), 332-358.

El-Moumen, A., Tarfaoui, M., & Lafdi, K. (2017). Mechanical characterization of carbon nanotubes based polymer composites using indentation tests. *Composites Part B: Engineering*, *114*, 1-7.

Geethamma, V. G., Kalaprasad, G., Groeninckx, G., & Thomas, S. (2005). Dynamic mechanical behavior of short coir fibre reinforced natural rubber composites. *Composites Part A: Applied Science and Manufacturing, 36*(11), 1499-1506.

Ghani, M. A. A., Salleh, Z., Hyie, K. M., Berhan, M. N., Taib, Y. M. D., & Bakri, M. A. I. (2012). Mechanical properties of kenaf/fibreglass polyester hybrid composite. *Procedia Engineering*, *41*, 1654-1659.

Godara, A., Gorbatikh, L., Kalinka, G., Warrier, A., Rochez, O., Mezzo, L., & Verpoest, I. (2010). Interfacial shear strength of a glass fibre/epoxy bonding in composites modified with carbon nanotubes. *Composites Science and Technology, 70*(9), 1346-1352.

Gupta, P., Chawla, V., Jain, V., & Angra, S. (2022). Green operations management for sustainable development: An explicit analysis by using fuzzy best-worst method. *Decision Science Letters, 11*(3), 357-366.

Halpin, J. C., & Tsai, S. W. (1967). Environmental factors in composite materials design. *US Air Force Technical Report AFML TR*, *67423*.

Hashemi, F., Brancheriau, L., & Tahir, P. M. (2018). Hybridization and yarns configuration effects on flexural dynamic and static properties of pultruded hybrid kenaf/glass fibre composites. *Composites Part A: Applied Science and Manufacturing*, *112*, 415-422.

Hine, P. J., Lusti, H. R., & Gusev, A. A. (2002). Numerical simulation of the effects of volume fraction, aspect ratio and fibre length distribution on the elastic and thermoelastic properties of short fibre composites. *Composites Science and Technology*, *62*(10-11), 1445-1453.

Idumah, C. I., & Hassan, A. (2016). Characterization and preparation of conductive exfoliated graphene nanoplatelets kenaf fibre hybrid polypropylene composites. *Synthetic Metals*, *212*, 91-104.

Idumah, C. I., Hassan, A., & Bourbigot, S. (2017). Influence of exfoliated graphene nanoplatelets on flame retardancy of kenaf flour polypropylene hybrid nanocomposites. *Journal of Analytical and Applied Pyrolysis, 123,* 65-72.

Iijima, S. (1991). Helical microtubules of graphitic carbon. *Nature, 354(6348),* 56-58.

Islam, M. S., Hasbullah, N. A. B., Hasan, M., Talib, Z. A., Jawaid, M., & Haafiz, M. M. (2015). Physical, mechanical and biodegradable properties of kenaf/coir hybrid fibre reinforced polymer nanocomposites. *Materials Today Communications*, *4*, 69-76.

Jangam, S., Raja, S., & Maheswar Gowd, B. U. (2016). Influence of multiwall carbon nanotube alignment on vibration damping of nanocomposites. *Journal of Reinforced Plastics and Composites*, *35*(8), 617-627.

Kari, S., Berger, H., & Gabbert, U. (2007). Numerical evaluation of effective material properties of randomly distributed short cylindrical fibre composites. *Computational materials science, 39*(1), 198-204.

Ku, H., Wang, H., Pattarachaiyakoop, N., & Trada, M. (2011). A review on the tensile properties of natural fibre reinforced polymer composites. *Composites Part B: Engineering*, *42*(4), 856-873.

Kumar, A., Angra, S., & Chanda, A. K. (2020). Analysis of the effects of varying core thicknesses of Kevlar Honeycomb sandwich structures under different regimes of testing. *Materials Today: Proceedings*, *21*, 1615-1623.

Kumar, N., Walia, R. S., & Angra, S. (2021). Study of mechanical properties of pultruded jute-glass reinforced unsaturated polyester bio-composites with hybrid filler loading. *World Journal of Engineering.*

Kumar, R., Kumar, K., & Bhowmik, S. (2014). Optimization of mechanical properties of epoxy-based wood dust reinforced green composite using Taguchi method. *Procedia Materials Science, 5,* 688-696.

Kwon, H. J., Sunthornvarabhas, J., Park, J. W., Lee, J. H., Kim, H. J., Piyachomkwan, K., Sriroth, K., & Cho, D. (2014). Tensile properties of kenaf fibre and corn husk flour reinforced poly (lactic acid) hybrid bio-composites: Role of the aspect ratio of natural fibres. *Composites Part B: Engineering, 56,* 232-237.

Lusti, H. R., Hine, P. J., & Gusev, A. A. (2002). Direct numerical predictions for the elastic and thermoelastic properties of short fibre composites. *Composites Science and Technology, 62*(15), 1927-1934.

Mishra, N., & Das, K. (2020). A Mori–Tanaka based micromechanical model for predicting the effective electroelastic properties of orthotropic piezoelectric composites with spherical inclusions. *SN Applied Sciences*, *2*(7), 1-14.

Mori, T., & Tanaka, K. (1973). Average stress in matrix and average elastic energy of materials with misfitting inclusions. *Acta metallurgica*, *21*(5), 571-574.

Parashar, S., & Chawla, V. K. (2021). A systematic review on sustainable green fibre reinforced composite and their analytical models. *Materials Today: Proceedings*, *46*, 6541-6546.

Parashar, S., & Chawla, V. K. (2022). Evaluation of fibre volume fraction of kenaf-coir-epoxy based green composite by finite element analysis. *Materials Today: Proceedings*, *50*, 1265-1274.

Prabhudass, J. M., & Palanikumar, K. (2021). Experimental investigation of Mechanical and Thermal properties of Coir-Kenaf reinforced epoxy composites. *Materials Today: Proceedings*, *44*, 3834-3837.

Ramesh, P., Prasad, B. D., & Narayana, K. L. (2020). Effect of fibre hybridization and montmorillonite clay on properties of treated kenaf/Aloevera fibre reinforced PLA hybrid nano-bio-composite. *Cellulose*, *27*(12), 6977-6993.

Rana, S., Bhattacharyya, A., Parveen, S., Fangueiro, R., Alagirusamy, R., & Joshi, M. (2013). Processing and performance of carbon/epoxy multi-scale composites containing carbon nanofibres and single-walled carbon nanotubes. *Journal of Polymer Research*, *20*(12), 1-11.

Rout, A., & Satapathy, A. (2012). Analysis of dry sliding wear behaviour of rice husk filled epoxy composites using design of experiment and ANN. *Procedia Engineering, 38,* 1218-1232.

Saba, N., Paridah, M. T., Abdan, K., & Ibrahim, N. A. (2016). Dynamic mechanical properties of oil palm nano-filler/kenaf/epoxy hybrid nanocomposites. *Construction and Building Materials, 124,* 133-138.

Sadik, Z., Ablouh, H., Benmoussa, K., Idrissi-Saba, H., Kaddami, H., & Arrakhiz, F. (2020). Use of 2D image analysis method for measurement of short fibres orientation in polymer composites. *Engineering Solid Mechanics, 8*(3), 233-244.

Sani, M. A., ABD LATIB, A. Z., Ng, C. P., Yusof, M. A., Ahmad, N., & Rani, M. A. M. (2011). Properties of coir fibre and kenaf fibre modified asphalt mixes. *Journal of the Eastern Asia Society for Transportation Studies*, *9*, 1274-1285.

Sapiai, N., Jumahat, A., & Mahmud, J. (2015). Flexural and tensile properties of kenaf/glass fibres hybrid composites filled with carbon nanotubes. *Jurnal Teknologi*, 76(3).

Saxena, T., & Chawla, V. K. (2021). Banana leaf fibre-based green composite: An explicit review report. *Materials Today: Proceedings, 46,* 6618-6624.

Saxena, T., & Chawla, V. K. (2022). Effect of fibre orientations and their weight percentage on banana fibre-based hybrid composite. *Materials Today: Proceedings*, *50*, 1275-1281.

Seidel, G. D., & Lagoudas, D. C. (2006). Micromechanical analysis of the effective elastic properties of carbon nanotube reinforced composites. *Mechanics of Materials*, *38*(8-10), 884-907.

Subasinghe, A., Somashekar, A. A., & Bhattacharyya, D. (2018). Effects of wool fibre and other additives on the flammability and mechanical performance of polypropylene/kenaf composites. *Composites Part B: Engineering*, *136*, 168-176.

Sudheer, M., Pradyoth, K. R., & Somayaji, S. (2015). Analytical and numerical validation of epoxy/glass structural composites for elastic models. *American Journal of Materials Science, 5*(3C), 162-168.

Tarfaoui, M., Lafdi, K., & El Moumen, A. (2016). Mechanical properties of carbon nanotubes-based polymer composites. *Composites Part B: Engineering, 103,* 113-121.

Theocaris, P. S., Stavroulakis, G. E., & Panagiotopoulos, P. D. (1997). Calculation of effective transverse elastic moduli of fibre-reinforced composites by numerical homogenization. *Composites Science and Technology*, *57*(5), 573-586.

Tsai, S. W., & Hahn, H. T. (2018). *Introduction to composite materials*. Routledge.

Yahaya, R., Sapuan, S. M., Jawaid, M., Leman, Z., & Zainudin, E. S. (2014). Quasi-static penetration and ballistic properties of kenaf–aramid hybrid composites. *Materials & Design*, *63*, 775-782.

Yusoff, R. B., Takagi, H., & Nakagaito, A. N. (2016). Tensile and flexural properties of polylactic acid-based hybrid green composites reinforced by kenaf, bamboo and coir fibres. *Industrial Crops and Products*, *94*, 562-573.

Zhao, Q., Tao, J., Yam, R. C., Mok, A. C., Li, R. K., & Song, C. (2008). Biodegradation behavior of polycaprolactone/rice husk eco-composites in simulated soil medium. *Polymer Degradation and Stability*, *93*(8), 1571-1576.